Highly accreting quasars at low and high redshift: a tool for cosmology?

P. Marziani[1], C. A. Negrete[2], D. Dultzin[2], M. L. Martinez-Aldama[3], A. Del Olmo[3], D. Esparza[2], M. D' Onofrio[4], J. W. Sulentic[3], G. M. Stirpe[5], E. Bon[6], N. Bon[6]

[1]INAF, Osservatorio Astronomico di Padova, Italy; [2]Instituto de Astronomía, UNAM, Mexico; [3]Instituto de Astrofísica de Andalucía (IAA-CSIC), Granada, Spain; [4]Università di Padova, Padova, Italia; [5]INAF, Osservatorio Astronomico di Bologna, Italia; [6]Belgrade Observatory, Serbia

Several new techniques (summarized in the Table aside) have been proposed in recent years to use quasars as redshift independent distance in indicators, with the goal of deriving Ω_M and Ω_Λ. **Highly accreting quasars** (xA for extreme accretors or extreme Population A) may literally be considered as "**Eddington standard candles**:" their Eddington ratio is expected to converge toward values of order unity, with small scatter. Using optical/UV spectral line widths as virial broadening estimators we are then able to derive black hole mass and a **"virial luminosity"** avoiding the use of scaling laws. **xA quasars are recognized from diagnostic ratios** in their rest-frame UV and optical spectra. The **Hubble diagram** with SDSS and dedicated Gran Telescopio Canarias (GTC) data is presented below. Mock samples show that the method can in principle provide significant constraints, especially on Ω_M if applied to z~2 quasars.

Sources	Parameters	Basic equation	Reference	Virial
extremely accreting quasars (xA)	Hard X-ray slope, velocity dispersion	$D_* = \frac{1}{\sqrt{4\pi}}\left[\frac{l_0(1+a\ln\dot{m}_{15}) f_{...} R_0}{G\kappa_0}\right]^{1/2(1-\alpha)} \frac{V^{...}}{F^{1/2}_{5100}}$	Wang et al 2013	V
extremely accreting quasars (xA)	[illegible] FWHM(Hβ) Eddington ratio = const	$L \propto \mathrm{FWHM(H\beta)}^4$	Marziani & Sulentic 2014	V
general quasar populations	X-ray variability, velocity dispersion	$\log\frac{L}{\mathrm{erg\,s^{-1}}} + 4\log\frac{\mathrm{FWHM}}{10^3\,\mathrm{km\,s^{-1}}} = \alpha\log\sigma^2_{rms} + \beta$	La Franca et al. 2014	V
mainly quasars at z<1	Reverberation mapping time delay τ	$\tau/\sqrt{F} \propto d_L$	Watson et al 2011, 2013; Czerny et al. 2013; Melia 2015	
general quasar populations	non linear relation between soft X and UV	$\log(F_X) = \Phi(F_{UV}, D_L) = \beta' + \gamma\log(F_{UV}) + 2(\gamma-1)\log(D_L)$	Risaliti & Lusso 2016	

"Eddington standard candles"

Recognizing highly accreting quasars

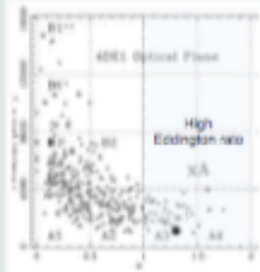

The optical, UV, and X properties of quasars can be organized on the basis of a few physical parameters, the most relevant of them being Eddington ratio, and to a second extent, orientation (Marziani et al. 2001). The Eddington ratio systematically changes along a sequence defined by FeII prominence [R_{FeII}= I(FeIIλ4570)/I(Hβ)] and FWHM of broad Hβ (the optical plane of the "eigenvector 1", figure on the left). The thick dot–dashed line separates extreme Pop. A sources by the criterion $R_{FeII} \geq 1.0$ from other spectral types. The large filled circle identifies the prototypical xA source I Zw 1. The optical criterion is found equivalent to an UV-based criterion: (a) I(AlIIIλ1860)/I(SiIII] λ1892)>0.5, (b) I(SiIII] λ1892)/I(CIII]λ1909)>1 which can be applied to high z quasars from optical observations.

We are presently carrying out an analysis of survey data and of data collected from dedicated observations at GTC to obtain high-S/N spectra of xA sources. At low z, ~ 80 spectra covering the Hβ range have been selected from the SDSS; 50 sources at redshift $2 < z < 4$ were observed with the OSIRIS camera at the GTC and cover the λ1900 Å blend. Examples of spectra and analysis are shown below.

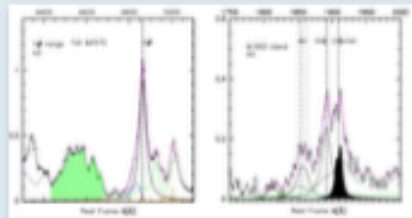

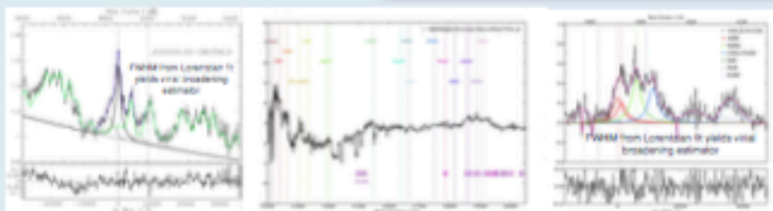

The virial luminosity equation

$$L \approx 7.8\,10^{44} \frac{\lambda^2_{Edd,1}\kappa_{0.5} f^2_{S,2}}{h\bar{\nu}_{i,100\,eV}} \frac{1}{(n_H U)_{10^{9.6}}} (\delta v)^4_{1000}\ \mathrm{erg\,s^{-1}},$$

It connects accretion luminosity to the line width (δv ~ FWHM of Hβ or of the intermediate ionization lines AlIIIλ1860 and SiIII]λ1892) through multiplicative terms that can be assumed to have a small dispersion around an average value L_0 for all xA sources, as a first approximation (in the following, we assume $\log L_0 = 44.79$ for the computation of the distance modulus μ). The equation was derived assuming virial motion, broad line region size scaling as $\propto L^{1/2}$, as well as a well-defined L/M ratio. It is the equivalent of the original Faber & Jackson (1976) relation linking the luminosity and velocity dispersion of galaxies.

The Hubble diagram

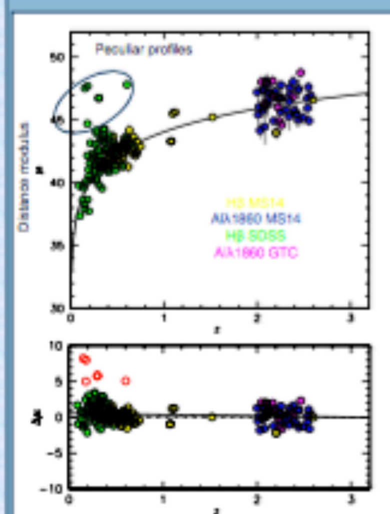

The diagram aside includes the 92 sources of Marziani and Sulentic (2014, MS14), and is supplemented by 79 new SDSS low-luminosity xA sources (green) and by 10 new high-z quasar observations with GTC (magenta). The sample rms is $\sigma_{\delta\mu} \approx 1.1$ (≈ 0.44 dex), not improved with respect to the previous work, due to the slightly larger scatter found among the low-luminosity sources. Some outlying quasars show peculiar profiles, and were excluded from the computation. The new data confirm the feasibility of the method, yielding a behavior consistent with concordance cosmology. **Significant results require an increase in sample size, reduction of intrinsic scatter and skew (believed to be associated with orientation effects, and non-virial motions due to outflows), and precise knowledge of the flux ratio at 5100 and 1800 Å, if Hβ and 1900 Å blend data are used together.**

Constraints on Ω_M from mock samples

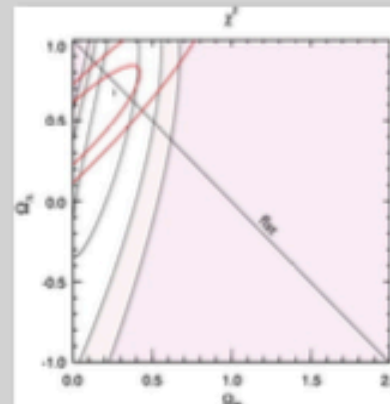

Comparison between the constraints set by the supernova photometric survey described by Campbell et al. (2013) (red lines) and an hypothetical mock sample of 400 quasars uniformly distributed in the range $0.1 < z < 3$, with rms = 0.3 that assumes concordance cosmology (shaded contours). Confidence intervals are at 1 and 2 σ for supernovae and 1, 2, 3 σ for the quasar mock sample. The flat geometry loci $\Omega_M+\Omega_\Lambda=1$ are also shown. Note the **potential ability of the quasar sample to better constrain Ω_M.** Only statistical errors are included in both cases. **A realistic application of the method requires a thorough understanding of the sources of systematic errors described in MS14, partly achievable through synoptic spectroscopic observations of the redshifted optical and UV spectral ranges.**

References

Campbell, H., et al. 2013, ApJ, 763, 88
Czerny, B., et al. 2013, A&A, 556, 97
Faber, S. M., Jackson, R. E., 1976, ApJ, 204, 668
La Franca, F., et al., 2014, ApJL, 787, L12
Marziani P., Sulentic J. MNRAS 442, 1211
Marziani, P., et al. 2001, ApJ, 558, 553
Melia, F. 2015, Ap&SS, 356, 34
Risaliti, G., Lusso, E., 2015, ApJ, 815, 33
Wang, J.-M., 2013, Phys. Rev. Lett., 110, 8
Watson, D., et al. 2011, ApJL, 149